Upper Frequency Limit of Flat Panel Loudspeakers - Evaluation of the Voice Coil Break-Up Modes

Benjamin Zenker[1], Sebastian Merchel[1], and M. Ercan Altinsoy[1]

[1]*Chair of Acoustics and Haptic Engineering, Dresden University of Technology, 01062 Dresden, Germany.*

Correspondence should be addressed to Benjamin Zenker (`benjamin.zenker@tu-dresden.de`)

ABSTRACT

During the monitoring of the behavior of different types of exciters attached to the same loudspeaker panel, significant deviations of the upper-frequency limit were discovered. These deviations depend on the resonance of the voice coil former and cannot be explained with the linear T/S parameters. This paper shows the indirect and direct measurement of the voice coil's break-up with two exemplary exciters. Furthermore, an FE-simulation model has been built to validate and visualize these break-up modes. Finally, a prototype with reinforced structure was constructed to increase the resonance frequency and to extend the frequency range of the loudspeaker panel.

1 Introduction

When the first measurements were made with a panel made out of mineral material and the exciter DAEX30HESF-4 (large voice coil), it was incorrectly assumed that the upper-frequency limit of the flat panel loudspeaker is described by the coincidence frequency of the panel. In this configuration with a 3 mm thick mineral panel and the exciter with the large voice coil, the frequency response is limited to 10 kHz.

During the monitoring of the behavior of different exciters attached to the same panel, significant deviations of the upper frequency limit were discovered. An example is shown in Figure 1. Two different exciters were mounted on a panel consisting of mineral material. The differences between both exciters can be described up to a specific frequency. After that specific frequency a strong resonance occurs, which limits the sound radiation. To identify the frequency-dependent differences individually, the graph in Figure 1 is subdivided into three sections:
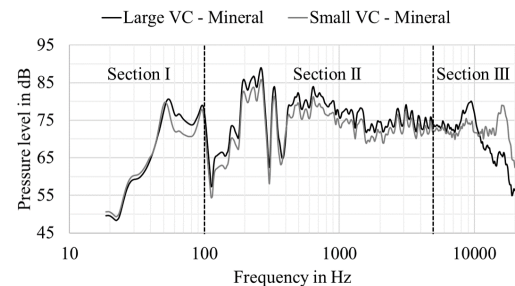

Fig. 1: SPL averaged response of two different Exciters mounted on the same panel subdivided in three sections

Section 1 has some differences which are explainable with the different resonance frequencies of the exciters and their individual moving magnet mass, which interacts with the first eigenmode of the membrane.

Section 2 shows two parallel graphs, where the shift is explainable with the different force resulting from the

Fig. 2: Examples of the chosen exciters with large voice coil and with small voice coil.

electrical voice coil resistance Re and force factor Bl. Section 3 shows a significant deviation of both graphs, which are not explainable with the difference of the moving mass of the voice coil Mms or the voice coil inductance Le. This corresponds more to a resonant behavior. The chosen exciters are shown in Figure 2. The exciter with large voice coil (VC) has a larger diameter and a longer VC compared to the exciter with the small VC. The mentioned resonance could be caused the different mechanical stiffness of the VCF or by a wavelength specific problem due to the different diameters of the VC. Both options are investigated in the following sections.

This paper presents several different ways of measuring and evaluating the upper frequency limit of an exciter. In chapter 2, the Thiele/Small parameters of two exciters will be analyzed, and conclusions are made regarding the estimated frequency limit. In addition to the driver resonance, an additional resonance occurs during the magnet measurement (with a fixed VC), which indicates a relationship with the upper-frequency limit. Chapter 3 shows the different acoustic behaviors of the exciters coupled to three various panels. In chapter 4, an FE-model of the exciter is developed to visualize the VC bending with different boundary conditions. A comparison of the simulation results and measurement data is presented to illustrate the accuracy of the simulation model. Chapter 5 presents an idea to suppress the bending of the voice coil former with a printed insert.

Measurements of the standard and modified exciter are made to visualize the influence of the reinforcement structure. In the last chapter, the different evaluation methods are compared according to accuracy, visualizability, and speed. This overview helps to evaluate the ways to analyze the upper-frequency limit of exciters. Furthermore, hints are given to shift the resonance of the VCF to higher frequencies during the design process of an exciter.

2   Linear parameter analysis

In the following chapter the Thiele/Small parameters of two exciters will be analyzed. The basic measurement setup for the measurement of T/S parameters is discussed and conclusions are made regarding the estimated frequency limit. Furthermore, the frequency dependent electrical impedance is measured, which is useful as an indicator for the voice coil resonance.

2.1   Measurement of T/S parameters

In comparison to a standard cone transducer, exciters have two degrees of freedom (DOF). The first DOF is the moving voice coil former (VCF), which is similar to a standard transducer without membrane. The eigenfrequency results from global stiffnes and the total mass consisting of voice coil former, voice coil (VC) and the plastic ring to glue the exciter. The second DOF the moving mass of the magnet. The eigenfrequency is the result of magnet mass and global stiffness. Both DOF need to be analyzed by fixing one DOF shown in Figure 3. In Table 1 the data of both measurement types is presented. It is visible that standard parameter Re, Le, Re_2, Le_2, Kms and Bl are nearly similar. They are independent of the measurement procedure. On the other hand Mms and fs are changing. The fs of the magnet measurement has higher importance to the whole flat panel loudspeaker. This driver resonance are able to interact with the first eigenmode of the membran, if the Mms is not attached to a frame and can move free. Therefore, it is always recommended to measure at least the magnet of an exciter. The high moving mass and the low eigenfrequency results in an interaction with the eigenmodes of the membrane. Furthermore, the eigenfrequency of the voice coil measurement is not meaniningful for the whole system, because of the strong influence of the membrane with high mass and high stiffness.

Table 1: T/S parameter of the choosen exciters measured at the voice coil (with fixed magnet) and at the magnet (with fixed voice coil).

Properties	DAEX30HESF-4 Large VC		DAEX25FHE-4 Small VC	
	VC	Magnet	VC	Magnet
Re [Ohm]	3.69	3.68	4.47	4.48
Le [mH]	0.14	0.15	0.10	0.11
Re2 [Ohm]	0.66	0.57	1.21	0.45
Le2 [mH]	0.09	0.10	0.07	0.07
fs [Hz]	307.1	32.3	203.2	27.5
Mms [g]	1.65	152.3	1.2	95.72
Kms [N/mm]	6.12	6.24	2.59	2.85
Bl [N/A]	5.11	5.03	3.92	3.95

2.2   Impedance measurement

Next to the T/S parameter, the frequency-dependent electrical impedance will be analyzed by using the Klippel LPM Module. The different results of the voice coil and magnet measurement of the electrical impedance are presented in Figure 4. By using the voice coil measurement, one peak of the eigenfrequency of each exciter is visible. By using the magnet measurement, two peaks in the electrical impedance curve become visible. The first is fs, the basis for T/S parameter calculation, and the result of the ratio of the moving mass of the magnet and global stiffness. The second peak fits the upper-frequency limit of the panel presented in Figure 1. This resonance is deliberately caused with the magnet measurement. Detailed investigations concerning
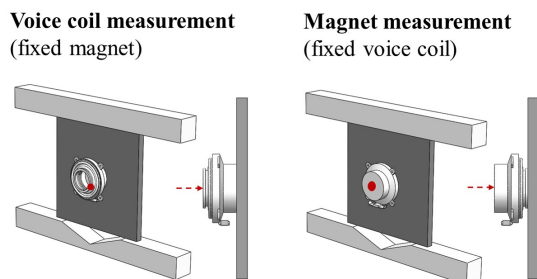
Voice coil measurement
(fixed magnet)

Magnet measurement
(fixed voice coil)

Fig. 3: Possibilities to evaluate the T/S parameter of an exciter. It is always recommended to measure at least the magnet displacement.

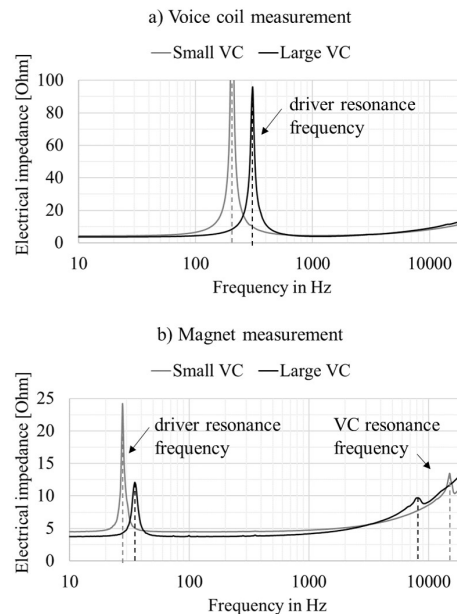this peak are discussed in the following chapters.

Fig. 4: Electrical impedance of two different exciters measured with voice coil and magnet measurement.

3   Acoustical measurement

To guarantee that the upper-frequency limit presented in Figure 1 is independent of the material properties, both exciters were analyzed with three different materials. The materials were chosen, based on their different propagation wavelength. This chapter presents the radiation results of both exciters mounted on three various panels.

3.1   Material selection

All material properties were calculated by using the modal analysis of a panel with free edges with an edge corner length of 400 mm x 400 mm. The material properties were fitted to the lowest frequency deviation of the measured modes in comparison to the calculated modes. Thickness and mass properties are fixed constraints and have not been changed for the fitting. The material parameters of the chosen materials are presented in Table 2. The materials were chosen based on the mineral material to have larger and smaller bending wavelength at the same frequency.

Table 2: Material parameters of the chosen panels to compare the resulting coincidence frequency

Properties		Mineral	Acrylic	HPL
Thickness [mm]	h	2.9	2.05	3.05
Young's mod. [GPa]	E	9.3	4.82	16.4
Density [Kg/m^3]	ρ	1595	1250	1480
Poissons ratio	v	0.32	0.32	0.3
Bending stiff. [Nm]	B	21.13	3.86	42.61
Area density [Kg/m^2]	m''	4.63	2.56	4.51
Coincidence [kHz]	f_c	8.76	15.27	6.09

The bending wavelength λ_b according to [1] is frequency-dependent and dependent to the bending stiffness B and mass per unit area m'' shown in Equation 1.

$$\lambda_B = \frac{2\pi}{\sqrt{\omega}} \left(\frac{B}{m''} \right)^{\frac{1}{4}} \qquad (1)$$

The used materials were chosen to have a larger and smaller bending wavelength compared to the mineral material. The coincidence frequency is selected as a comparison value, the frequency for which $\lambda_b = \lambda$ or $c_b = c$. This condition of equal wavelengths in the panel and in air is termed as wave coincidence. It will be calculated from Equations 1 and 2 and results in the Equation 3 to calculate the coincidence frequency f_{coin}.

$$\lambda_A = \frac{c_A}{f} \qquad (2)$$

$$f_{coin} = \frac{c_A^2}{2\pi} \sqrt{\frac{m''}{B}} \qquad (3)$$

If the wavelength of the sound in air is greater than the wavelength of the sound in the plate, no wave coincidence can occur. The coincidence frequency f_{coin} is defined as the lowest frequency at which wave coincidence occurs. Under this condition, the panel vibrates with an amplitude, which is almost equal to the amplitude of the air particles in the incident wave. In other words, the panel radiates a wave (the transmitted wave) that is almost as intense as the exciting wave (the incident wave) — this results in very efficient radiation. At the coincidence frequency, f_{coin} the radiating angle is 90 deg, which will decrease to higher frequencies.
The acrylic panel has much lower B to m'' ratio which results in a smaller bending wavelength at the same

frequency and a higher coincidence frequency. The HPL (high pressure laminate) is much stiffer compared to the mineral material and results in higher bending wavelength and a lower coincidence frequency.

3.2 Measurement setup

All acoustical measurements were performed at the anechoic chamber at the Technical University Dresden with the following equipment:

- Microphone: Gras 40HL (Low-noise)
- Power Module: Gras 12AK
- Measurement system: Klippel DA2
- Turntable: LinearX LT360
- Software operations: Robotics and TRF.

It is known that the directivity pattern of a flat panel loudspeaker is strongly dependent on the angle [2]. Therefore, it is always recommended analyzing flat panel speakers more than at a single point. The measured distance is 2 m and all levels are referenced to 1 m distance. The applied smoothing is 1/20 per octave. The microphone was placed to the center of the panel. The radiation in horizontal plane is measured by using a fixed microphone and the loudspeaker is placed on a rotating table. An average of the individual pressure values in horizontal plane with 10 deg resolution gives a sufficiently fine resolution compared to a single point measurement [3]. The angle averaged pressure will be calculated from the angle dependent pressure $\tilde{p}_{k,\theta}$ with Equation 4, where T is the number of angles measured:

$$\tilde{p}_{AVG}(f) = \sqrt{\frac{1}{T} \sum_{t=1}^{T} (\tilde{p}_\theta(f))^2} \qquad (4)$$

which can be written as

$$SPL_{AVG}(f) = 20 \cdot log_{10} \left(\frac{\tilde{p}_{k,AVG}(f)}{p_0} \right) dB. \qquad (5)$$

3.3 Acoustical results

The acoustic results of the different exciters mounted on three various panels are presented in Figure 5 and 6. The magnitude in Figure 5 is normalized to the mean SPL of 80 dB to eliminate the effect of the more powerful motor. Figure 5 visualizes the different coincidence frequencies for the three materials, which fit with the
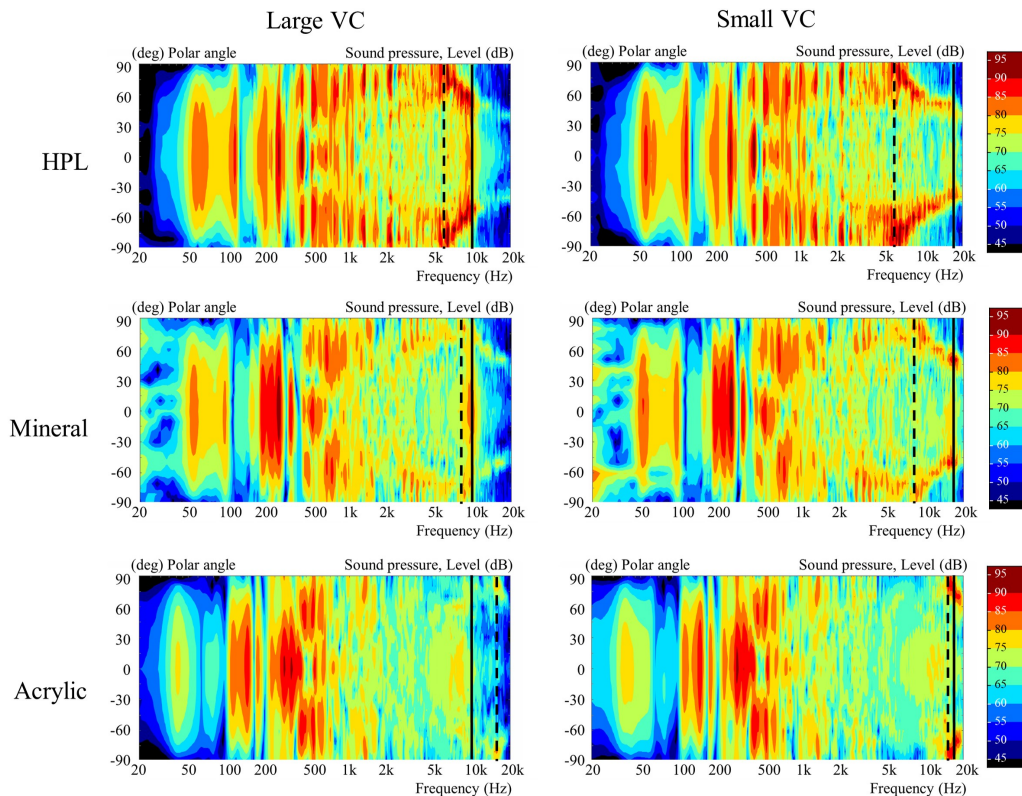
Large VC   Small VC

Fig. 5: Radiation pattern of three different panels normalized to the mean SPL of 80 dB excited with two different exciters. The dashed line marks the coincidence frequency. The bold line marks the frequency limit.

results in Table 2. Above the coincidence frequency the efficient radiation angle decreases and the sound is beamed frequency-dependent in different directions. However, the upper frequency limit of each panel is independent of the material properties, it is an exciter specific problem. The effect is best demonstrated with the HPL panel. Coincidence starts at 6.1 kHz and both exciters have a strong off-center radiation. The exciter with large VC is limited to 9 kHz and the sound pressure level decreases above this frequency compared to the exciter with smaller VC. For the Large VC exciter it is not possible to radiate to higher frequencies with a sufficient amplitude. Right before this frequency limit a resonance is generated which is exciter specific. This resonance is panel independent. The exciter with large VC is is limited at 8 - 9 kHz and the exciter with small VC at 14 - 16 kHz. Due to the small frequency difference of coincidence of the mineral panel and the voice coil resonance the exciters (with large VC), it was incorrectly assumed that the upper-frequency limit

is described by the coincidence frequency of the panel. However, it could be shown that this frequency limit is exciter specific. Compared due to the break-up of the membrane of pistonic loudspeakers the SPL will decrease significantly after the break-up [4].
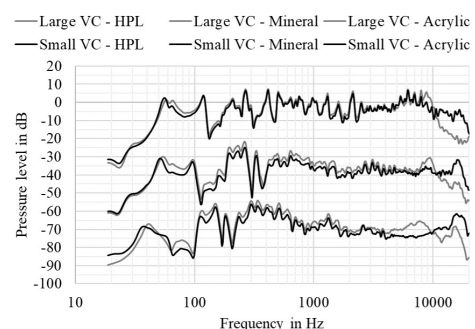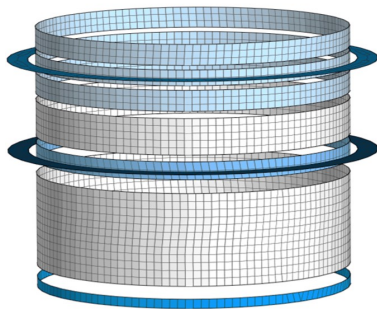

Fig. 6: $SPL_{AVG}(f)$ of all panels referenced to their mean SPL and shifted 20 dB.

Color	Name	Material layup	DOF Trans			DOF Rot		
			X	Y	Z	X	Y	Z
1	VCF + VC	0.15mm Kapton 0.25mm copper						
2	VCF	0.15mm Kapton						
3	VCF + SPY	0.15mm Kapton						
4	VCF + MS	0.15mm Kapton 1.0mm PE						
5	EI	Electrical impedance						
6	MI	Mechanical impedance						

Fig. 7: FE-model of the voice coil former of the exciter with large voice coil. All individual subsystems are marked in different colors and shifted to maintain the overview throughout the model.

4 Simulation model

In this chapter the simulation model will be introduced and the impedance and force modeling described. The simulation results will be compared with measurement data and the displacement behaviour visualized.

4.1 Simulation model

The VCF was modelled in the simulation software wave6 [5]. All applied impedances are based on the electro-mechanical equivalent circuit of a lumped parameter model of an electro-dynamical transducer [6]. The VCF can be abstracted as a 2D-cylinder shell, which is subdivided in several FE-systems with different material layups and constraints. The model layout is presented in Figure 7. The first area represents the VC made from copper and the Kapton VCF. The properties of the chosen material for the VCF and VC are presented in Table 3 and are based on the datasheets of DuPont[7] and Dolbow and Gosz [8]. The layup for this area consists of 0.15 mm Kapton and 0.25 mm Copper. It has all degree of freedom and is not limited or leaded. The second part is the VCF with a thickness of 0.15 mm, which exists twice in the model. The third part specifies the area of the spider, where translation in x and y-direction and rotations about the z-axis are limited.

A detailed view of the force and impedance modeling is given in Figure 8. The force is introduced via rigid body elements (RBE) from an electro-mechanical equivalent circuit, which is coupled in z-direction. In this case RBE2 were chosen, to couple the movement of a single of independent node to a group of dependent nodes. The force is introduced as 1N in the FE-system
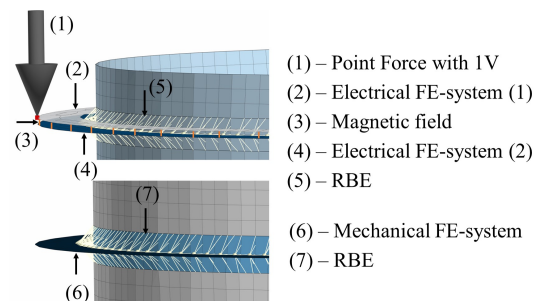

(1) – Point Force with 1V
(2) – Electrical FE-system (1)
(3) – Magnetic field
(4) – Electrical FE-system (2)
(5) – RBE
(6) – Mechanical FE-system
(7) – RBE

Fig. 8: Visualization of the force and impedance modeling: The electrical and mechanical impedance are coupled with RBE to the cylinder.

(1), which represents the electrical part and 1V input. Electrical FE-system (1) and (2) are coupled via a transfer impedance, which represents the magnetic field and the transformation from electrical flux to mechanical movement. The induced Lorentz force transferred as a resulting velocity in the electrical FE-system (2) and coupled via RBE2 in z-direction to the 1.5 mm FE-ring of the cylinder. Furthermore, the stiffness of the driver suspension is applied as a frequency dependent boundary impedance to the mechanical FE-system, which is coupled via RBE in z-direction to the cylinder.

Table 3: Material parameters of the VC and VCF

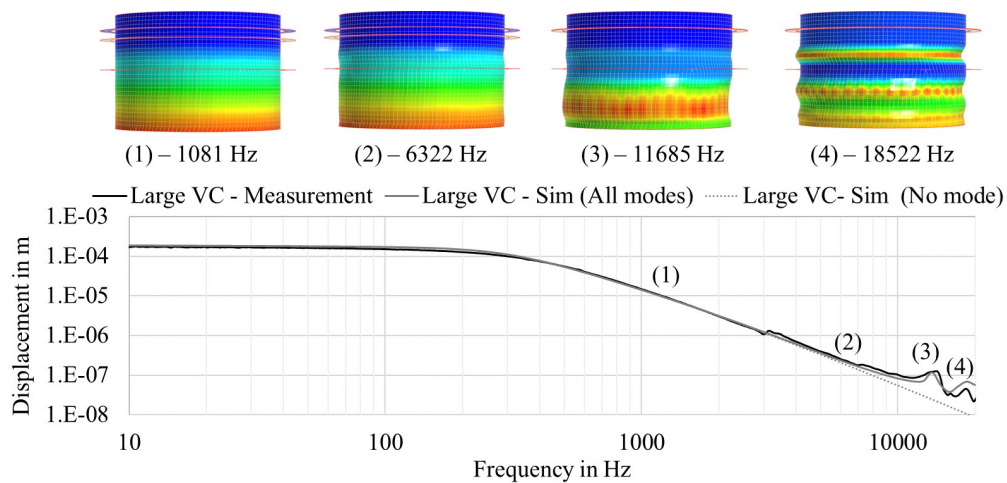| Properties		Kapton HN	Copper
Young's mod. [GPa]	E	2.76	128
Density [Kg/m^3]	ρ	1420	8960
Poissons ratio	ν	0.34	0.36

Fig. 9: Top: Visualization of the voice coil former displacement at different frequencies.
Bottom: Measured and simulated averaged magnitude of the transfer function H(f) of the voice coil displacement of the exciter with large voice coil and free boundary conditions.

4.2 Evaluation with the voice coil measurement

All measurements were performed at the Technical University Dresden with following equipment:

- Laser: Keyence LK-H052 (High-Accuracy)
- Measurement system: Klippel DA3
- Software operations: TRF.

Since the displacements are very small (in the range of 1.0E-07 m), the whole setup requires cautiousness. To achieve a sufficient signal to noise ratio, the signal was shaped (-40 dB below 300 Hz and -20 dB below 1 Hz) to apply 8 Vrms for a short amount of time at high frequencies. Additionally the measurement was averaged 256 times and the frequency resolution was reduced to 11.72 Hz linear space, which is still enough for high frequencies.

In the following section, the evaluation of the magnitude of the VC displacement in the normal direction with fixed magnet and side displacement with fixed VC was chosen. Figure 9 compares simulated and measured averaged magnitude of the transfer function H(f) of the VC displacement for the exciter with large voice coil and free boundary conditions. The averaging is performed via eight evenly distributed points on the surface. Figure 9 shows a good fit between the simulation and measurement results. Furthermore, a model with no modal extraction was built to visualize the influence

of the bending on the VC displacement. Above 6 kHz, the impact of the bending is getting more important and the displacement increases compared to an ideal stiff cylinder shell. This frequency dependent movement is also presented in the top part of Figure 9. Below 6 kHz the cylinder behaves as an ideal cylinder and moves just in z-direction without any bending. Above 6 kHz a bending of the VCF is starting, which gets more complex at higher frequencies. The movement at 11.7 kHz and 18.5 kHz demonstrates an additional bending in the upper part of the cylinder. The voice coil measurement is only an indicator for resonances and helps to visualize the deviations from an ideal structure. The exact frequency of the voice coil resonance is not detected. However, it is essential to note that this bending is caused in air, and therefore this resonance could also occur in conventional drivers.

Fig. 10: Measurement of the side VCF displacement.

4.3 Evaluation with the magnet measurement

Chapter 4.2 has shown, that the exact frequency of the voice coil resonance is not detectedable. This frequency is obtained by the magnet measurement method, where the bending of the VCF is systematically generated. The bending is measurable on the side of the exciter shown in Figure 10.

This situation can also be created in the simulation model. It is necessary to block the DOF of the system. For this purpose the boundary conditions of the front of the exciter (the point, where the VCF and the membrane meet) are fixed and all DOF are blocked. The results of this evaluation method are shown in Figure 11. The measurement has been performed with the same properties as the voice coil measurement. The simulation model has not changed, except for the boundary conditions. Figure 11 shows a good fit of the simulation and measurement results in the area of the resonance. Below the resonance the structure bends frequency independent. The measurement results show a deviation at low frequencies which are due to noise and other movements of the exciter and the test stand. Above the resonance the structure bending decreases and and higher order modes are excited.

It can be concluded that the voice coil former starts to bend at the voice coil resonance frequency, and therefore the energy in the panel decreases. This VCF bending and the resulting VC break-up explains the SPL loss above the VC resonant frequency.
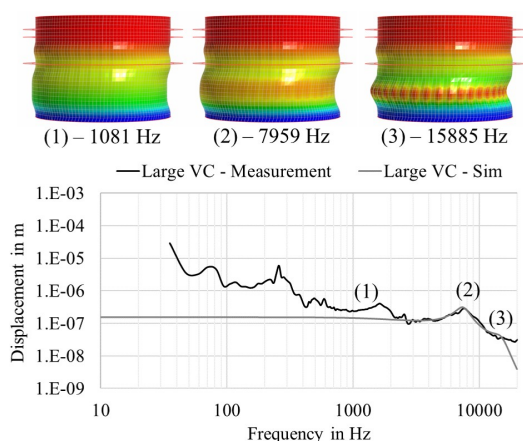

(1) – 1081 Hz   (2) – 7959 Hz   (3) – 15885 Hz

Fig. 11: Averaged magnitude of the transfer function H(f) of the side displacement of the exciter with large voice coil (LVC) and fixed boundary conditions.
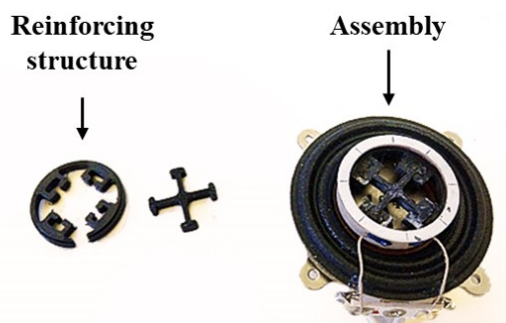

Fig. 12: Reinforcing structure and assembly of the optimized prototype with reinforcing structure to suppress the bending of the VCF

5 Analysis of an reinforced prototype

To verify the assumption that the frequency limit is represented by the VC breakup, the bending is suppressed by an additional reinforcement strcuture. This structure was printed to enable subsequent integration and free movement of the voice coil. It is designed like a spring, which can be stabilized by the additional cross. The structure was glued in with cyanoacrylate.

It shall be shown that the resonance frequency of the exciter is shifted to higher frequencies and the frequency limit is determined by the bending. It is to be expected that the shift of the resonance is not too large, because the exciter has buckled in the upper part of the VCF.

To confirm the reinforcement of the VCF, the measurement of the electrical impedance as well as the sound radiation, is performed with the modified exciter.

The measurement of the electrical impedance in the magnet configuration shows that the second resonance was increased from 8 kHz to 10 kHz. This confirms that the resonance is due to the bending of the cylinder and that reinforcement shifts the eigenfrequencies of the cylinder to higher frequencies. Additionally, it is confirmed that no change of the first resonance occurs during the magnet measurement because no mass of the magnet and stiffness of the suspension was changed. Despite the large reinforcing structure, the new cut-off frequency of 10 kHz is still very low. This is due to bending in the higher part of the cylinder, which cannot be corrected by the introduced reinforcing structure.

By comparing the averaged frequency responses in Figure 14, the impact of the reinforcement is confirmed. All panels have a higher cut-off frequency as a result of the shifted VCF resonance. The frequency responses
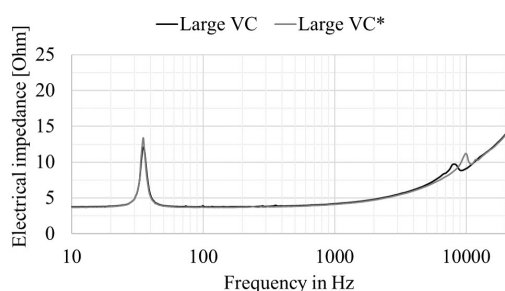
Fig. 13: Electrical impedance of the exciter with reinforced structure Large VC* and in standard configuration Large VC.

remain nearly equal, except for a small resonance between 4 kHz and 6 kHz. The additional mass of the reinforcing structure doubles the moving mass of the voice coil of the exciter, which has a small influence on the SPL at higher frequencies. If the moving mass of the panel is large, e.g. with mineral or HPL material, the decrease in SPL due to the increased moving mass is not noticeable.

Therefore, it is not needed to reduce the moving mass of the voice coil system of the exciter in the same way like standard pistonic loudspeakers. The moving mass of the voice coil system is determined by the mass of the VC. An increase of the VCF mass by increasing the thickness or using a the material with higher Young's modulus e.g. Aluminium would not change the sensitivity of the whole system, but would help to increase the usable frequency range of the exciter.
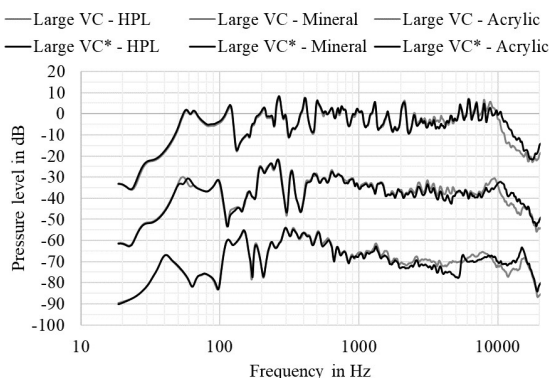

Fig. 14: $SPL_{AVG}(f)$ of all panels referenced to their SPL_{mean} and shifted by 20 dB excited with the large and modified exciter VC*.

6 Summary

The following paper presents the influence of the voice coil break-up due to the upper-frequency limit of a bending wave loudspeaker. This frequency limit is independent of the panel and its properties. The frequency limitation is only caused by the stiffness properties of the voice coil of the exciter. Break-up modes are known from pistonic loudspeaker and represent the limit of the rigid body movement of the membrane. This effect happens at high frequencies and can be used to increase the efficiency of a loudspeaker [4, 9]. This study presents the break-up of the voice coil former, which results also in peak in the sound pressure level. But compared due to the break-up of the membrane the sound pressure level will decrease significantly after the break-up. This is due to the reason that the VCF is no longer rigidly coupled to the membrane.

To identify the voice coil break-up to, several ways were presented. An overview of all methods are shown in Table 4, whereby the accuracy of the frequency analysis for the upper-frequency limit, the visualizability of the mode shape of the voice coil resonance, and the required time to obtain the results are rated for all methods.

Table 4: Comparison of different analysis methods based on the criteria accuracy, visualizability, and speed.

Method	Accuracy	Vis.	Speed
Impedance (VC fixed)	++	- -	++
Sound pressure level	+	−	+
Laser VC (magnet fixed)	- -	- -	o
Laser magnet (VC fixed)	+	- -	o
Laser side (VC fixed)	+	o	o
Simulation model	++	++	- -

The electrical impedance measurement (in magnet configuration) has proven to be the most effective one. The natural resonance of the voice coil former can be detected in the impedance curve via the frequency-dependent impedance. The shape of the bending is not detected. This fact is more important for an exciter producer, compared to the loudspeaker designer. For them, only the upper frequency limit is relevant.

Another possibility is to determine the frequency limit by measuring the sound pressure level. Independent of

the panel, the upper-frequency limit becomes visible by a strong level decreasing. It is detectable in the simplest case by an on-axis measurement or with an averaged measurement in horizontal plane.

Furthermore, it is possible to detect the bending with a laser. This detection requires a precise laser and high-class measurement equipment. With a very high number of averaging and a shaped signal, the resonance can be detected. Two methods were shown, whereby the voice coil measurement method only gives an indication of resonances, but the exact frequency of the voice coil resonance is not detected. This frequency is obtained by the magnet measurement method, where the bending of the VCF is systematically generated. However, it is essential to note that this bending is caused in air, and therefore this resonance could also occur in conventional drivers.

As the most sophisticated solution, the modeling with an acoustic FE-tool has proven to be the best for visualizability. The precise modeling requires most of the time in preparation. However, based on a working simulation model, several parameters can be estimated and visualized, such as the influence of wall thickness, Young's modulus, or diameter. This enables detailed optimization of the exciter structure.

However, it is recommended to stiffen and strengthen the space between the top of the voice coil winding to the exciter front (the point, where the VCF and the membrane meet). While the voice coil winding stack provides the mechanical integrity to the voice coil assembly, the space between the top of the coil winding and the front can bend. This limits the highest frequency of the exciter and the flat panel loudspeaker. The following design criteria are recommended to increase the stiffness of the VCF:

- Increasing the Young's modulus of chosen material of the VCF

- Increasing the thickness of the VCF

- Decreasing the length of the VCF

- Decreasing the diameter of the VCF

- Using local reinforcement

- Changing the position of the attachment of the spider to the VCF.

As a next step, the proposed reinforcement options can be compared against each other in terms of effectiveness, practical usability, and costs. Furthermore, based on this study, new exciter designs with particularly strong voice coil formers are conceivable to extend the usable frequency range of flat panel loudspeakers to highest frequencies.

References

[1] Fahy, F. and Gardonio, P., *Sound and structural vibration: Radiation, transmission and response*, Elsevier/Academic, Amsterdam and London, 2nd ed. edition, 2007, ISBN 978-0-12-373633-8.

[2] Zenker, B., Merchel, S., and Altinsoy, M. E., "Rethinking Flat Panel Loudspeakers—An Objective Acoustic Comparison of Different Speaker Categories," in *Audio Engineering Society Convention 147*, 2019.

[3] Zenker, B., Rawoof, S. S. A., Merchel, S., and Altinsoy, M. E., "Low Deviation and High Sensitivity—Optimized Exciter Positioning for Flat Panel Loudspeakers by Considering Averaged Sound Pressure Equalization," in *Audio Engineering Society Convention 147*, 2019.

[4] Cardenas, W., "Modelling and Measurement of Nonlinear Intermodal Coupling in Loudspeaker Diaphragm Vibrations," Audio Engineering Society, 2019.

[5] wave6, "Software version 2019.11.2," Dassault Systemes SIMULIA Corporation, available at www.wavesix.com.

[6] Seidel, U. and Klippel, W., "Fast and Accurate Measurement of the Linear Transducer Parameters," Audio Engineering Society, 2001.

[7] DuPont, "DuPont-Kapton-HN-datasheet," in *https://www.dupont.com/content/dam/dupont/products-and-services/membranes-and-films/polyimde-films/documents/DEC-Kapton-HN-datasheet.pdf*, "DuPont Corporation", Accessed 6th of January 2020.

[8] Dolbow, J. and Gosz, M., "Effect of out-of-plane properties of a polyimide film on the stress fields in microelectronic structures," *Mechanics of Materials*, 23(4), pp. 311–321, 1996.

[9] Klippel, W., "Green Speaker Design (Part 1: Optimal Use of System Resources)," in *Audio Engineering Society Convention 146*, 2019.